Master equation approach to computing RVB bond amplitudes

K. S. D. Beach
Institut für Theoretische Physik, Universität Würzburg, Am Hubland, 97074 Würzburg, Germany
(Dated: September 20, 2007)

We describe a "master equation" analysis for the bond amplitudes $h(\mathbf{r})$ of an RVB wavefunction. Starting from any initial guess, $h(\mathbf{r})$ evolves—in a manner dictated by the spin hamiltonian under consideration—toward a steady-state distribution representing an approximation to the true ground state. Unknown transition coefficients in the master equation are treated as variational parameters. We illustrate the method by applying it to the J_1–J_2 antiferromagnetic Heisenberg model. Without frustration ($J_2 = 0$), the amplitudes are radially symmetric and fall off as $1/r^3$ in the bond length. As the frustration increases, there are precursor signs of columnar or plaquette VBS order: the bonds preferentially align along the axes of the square lattice and weight accrues in the nearest-neighbour bond amplitudes. The Marshall sign rule holds over a large range of couplings, $J_2/J_1 \lesssim 0.418$. It fails when the $\mathbf{r} = (2, 1)$ bond amplitude first goes negative, a point also marked by a cusp in the ground state energy. A nonrigourous extrapolation of the staggered magnetic moment (through this point of nonanalyticity) shows it vanishing continuously at a critical value $J_2/J_1 \approx 0.447$. This may be preempted by a first-order transition to a state of broken translational symmetry.

I. INTRODUCTION

In the early 1970s, a resonating-valence-bond (RVB) wavefunction[1] with nearest-neighbour (NN) bonds only was proposed as a possible ground state for the quantum Heisenberg model on the triangular lattice.[2,3] This short-ranged, quantum-disordered[4,5] RVB state was conceived in analogy with the spin liquid state found in one dimension.[6,7] The belief was that classical 120° Néel order was unlikely to survive in the presence of strong quantum fluctuations.

This conjecture ultimately proved incorrect. Like other low-coordination-number antiferromagnets,[8,9] the triangular system is ordered at zero temperature.[10,11,12] Consequently, its ground state cannot be described in a basis of short bonds. One can show, in fact, that a correct description must involve valence bonds on all length scales.[13]

A generalization of the RVB state that includes long bonds was later proposed by Liang, Doucot, and Anderson for use as a variational wavefunction in the square-lattice Heisenberg model.[14] Their idea was to factorize the weight associated with each valence bond configuration into a product of individual bond amplitudes that depend only on the vector $\mathbf{r}$ connecting bond endpoints. Unlike the NN-bond RVB, which is unique, the long-range version is a family of states parameterized by the bond distribution function, $h(\mathbf{r})$. In $d = 2$, the RVB wavefunction has expressive power to describe both an antiferromagnetically ordered phase and a featureless quantum disordered phase.[14,15] It may be a good variational wavefunction for systems in which antiferromagnetism is killed by the addition of frustrating interactions.

As a practical matter, optimizing the bond amplitudes numerically is not straightforward. The number of independent parameters is of the order of the system size, and the energy depends only very weakly on the amplitudes of the longest bonds. Thus, obtaining well-converged results becomes increasingly difficult for large lattices, and scaling to the thermodynamic limit is unreliable. Lou and Sandvik[16] have made some progress by experimenting with different optimization schemes. They recently carried out an unbiased variational determination of $h(\mathbf{r})$ for the square-lattice Heisenberg model and were able to achieve lattice sizes up to 32×32.

Liang, Doucot, and Anderson circumvent the problems associated with a macroscopic number of degrees of freedom by assuming a functional form for $h(\mathbf{r})$. They vary the amplitudes of only a few short bonds and fix the remainder under the assumption of a radially symmetric bond-length distribution and algebraic decay at long distances.[14] For local, nonfrustrating interactions, this assumption turns out to be essentially correct.[17] Nonetheless, their choice of functional form is *ad hoc*, and there is nothing in their approach that provides insight into how the amplitudes might change when competing interactions are introduced.

In this paper, we describe an alternative method for calculating the bond amplitudes that requires at most a few variational parameters. The utility of the method is tested by applying it to the J_1–J_2 model. As in Ref. 14, we make strong assumptions about the form of the bond distribution. In our case, however, the choice of functional form for $h(\mathbf{r})$ is guided by a master equation that mimics the reconfiguration of bond amplitudes induced by the evolution operator.

The J_1–J_2 model describes a system of spin-half moments arranged on a square lattice in which Heisenberg interactions of strength J_1, acting along the plaquette edges, compete with frustrating interactions of strengh J_2, acting across the plaquette diagonals. At $J_2/J_1 = 0$ and $J_2/J_1 = \infty$, the model has two- and four-sublattice Néel order, respectively. There is a gapped intermediate phase in the vicinity of $J_2/J_1 \approx 0.5$, whose exact nature remains controversial. There has been speculation about a possible spin liquid state,[19,20,21,22,23] but a state with broken translational symmetry now seems more likely. The leading candidate is a valence bond solid (VBS) with

either columnar[24,25,26,27] or plaquette[28,29,30] order.

The extent of the intermediate phase has been determined to about one digit of precision. Exact diagonalization on small clusters[31] puts the lower critical point at $J_2/J_1 = 0.34(4)$, but this appears to be an underestimate. Bond operator calculations[32,33] based on the columnar VBS predict $0.38 \lesssim J_2/J_1 \lesssim 0.62$ for the region of stability, and series expansions[34,35] from the magnetic side give $0.4 \lesssim J_2/J_1 \lesssim 0.6$. A quantum Monte Carlo study,[36] in which stochastic reconfiguration is used to partially alleviate the sign problem, reports a transition to a gapped state at $J_2/J_1 \approx 0.4$.

It has been established from energy level crossings in series expansion that the transition at the upper critical point is first order.[37] No such crossings have been detected at the lower critical point, at least within the numerical accuracy that can be achieved. In most of the studies cited above, it is implicitly assumed that the transition at the lower critical point is second order. If that is true—and if the intermediate phase is indeed bond ordered—then the lower critical point may constitute a deconfined quantum critical point, as envisioned by Senthil *et al.*[38]

The fact that bond operator methods indicate a high density of triplet modes near a deconfined quantum critical point,[39] but only a low density near the critical point of the J_1–J_2 model,[32] leaves room for doubt. Indeed, a recent series expansion study points to a *first order* transition at $J_2/J_1 \approx 0.43$ on the basis of an energy functional computed for a fictitious translational-symmetry-breaking field.[40] This is supported by the argument due to Chubukov[41] that a continuous transition is only possible when a third-nearest-neighbour interaction $J_3 > 0$ is present.

The results reported here cannot settle this question with any certainty, but they do appear to be more consistent with a first order Néel–VBS transition.

II. MASTER EQUATION FOR FACTORIZABLE RVB BOND AMPLITUDES

The spin-rotation-invariant (total spin $S = 0$) ground state of a system of $2N$ spin-$\frac{1}{2}$ moments can be written as a superposition of valence bond states.[42,43] The simplest RVB ansatz is to assume that the weight given to each bond configuration is a product of individual bond amplitudes:

$$|h\rangle = \sum_v \left[\prod h(\mathbf{r})\right]|v\rangle. \tag{1}$$

Here the sum is over all partitions of the lattice into N singlet pairs, and the product is over all vectors $\mathbf{r}$ drawn between valence bond endpoints. [Anderson's NN-bond RVB corresponds to $h(\mathbf{r}) = \delta(|\mathbf{r}|-1)$.] In the special case of a nonfrustrated model on a bipartite lattice, the amplitudes $h(\mathbf{r})$ are real and nonnegative and strictly zero whenever $\mathbf{r}$ connects valence bonds in the same sublattice. See Fig. 1. This is just a restatement of the Marshall sign theorem.[44]

FIG. 1: Spins on the A sublattice (solid circles) and B sublattice (open circles) are grouped into pairs forming singlets. Each pairing configuration is characterized by a set of directed bonds connecting A sites to B sites.

One way to compute the $h(\mathbf{r})$ values appropriate for a given model is to consider the τ-dependent family of states

$$|h(\tau)\rangle = e^{-\tau\hat{\mathcal{F}}\hat{H}\hat{\mathcal{F}}}|h(0)\rangle, \tag{2}$$

where $\hat{H}$ is the hamiltonian of interest and $\hat{\mathcal{F}}$ is an operator that projects onto the space of factorizable RVB wavefunctions. In each time step $d\tau$, some fraction of the bond amplitude is reapportioned as bonds are created and destroyed. Correlations between bonds that go beyond the RVB framework are prevented from accumulating. This process is governed by a master equation that describes how the distribution $h(\mathbf{r})$ evolves towards its steady-state solution. Note that the wavefunction that emerges in the $\tau \to \infty$ limit is not strictly equal to the projection $\hat{\mathcal{F}}|\psi\rangle$ of the true ground state $|\psi\rangle$; nor is it equal to the variationally determined state $|h\rangle$ that minimizes $E = \langle h|\hat{H}|h\rangle/\langle h|h\rangle$. Nonetheless, all three are very similar to one another.[45]

The key observation is that the valence bond basis is closed under operation by the Heisenberg interaction. Operating on an existing bond simply leaves the bond as is [and the distribution $h(\mathbf{r})$ unchanged] whereas operating between two bonds maps them to their complementary tiling:

$$\Big(\frac{1}{4} - \mathbf{S}_i \cdot \mathbf{S}_j\Big)[i,j] = [i,j], \tag{3}$$

$$\Big(\frac{1}{4} - \mathbf{S}_i \cdot \mathbf{S}_j\Big)[i,l][k,j] = \frac{1}{2}[i,j][k,l]. \tag{4}$$

Here $[i,j] = \frac{1}{\sqrt{2}}(|\uparrow_i\downarrow_j\rangle - |\downarrow_i\uparrow_j\rangle$ denotes a singlet formed from the spins at sites i and j. The effect of Eq. (4) is depicted in Fig. 2.

For the NN Heisenberg model on a d-dimensional (hyper-)cubic lattice, the master equation is

$$\dot{h}(\mathbf{r}) = \sum_{\mathbf{a}}\big[\delta_{\mathbf{r},\mathbf{a}} + \sum_{\mathbf{r}',\mathbf{r}''}\delta_{\mathbf{r}'+\mathbf{r}''-\mathbf{a},\mathbf{r}}h(\mathbf{r}')h(\mathbf{r}'')\big] - 2zh(\mathbf{r}), \tag{5}$$

where $\dot{h} = \partial h/\partial\tau$, $z = 2d$ is the coordination number, and $\mathbf{a}$ ranges over all NN vectors. This is correct only insofar as $h(\mathbf{r})$ accurately measures how often a bond of

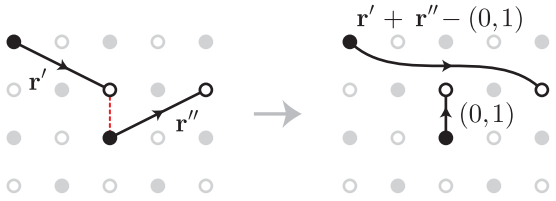

FIG. 2: A nonfrustrating Heisenberg interaction, indicated by the dotted (red) line, is applied between sites in opposite sublattices. The resulting reconfiguration creates one valence bond where the interaction was applied and another between the two remaining endpoints.

type $\mathbf{r}$ appears in the superposition of valence bond configurations making up the RVB state. Geometrical tiling constraints, which are increasingly important at low coordination number, have been ignored. Nonetheless, this level of approximation allows us to proceed analytically.

Equation (5) conserves the unit normalization of the total weight:

$$\sum_{\mathbf{r}} \dot{h}(\mathbf{r}) = z + z\left[\sum_{\mathbf{r}} h(\mathbf{r})\right]^2 - 2z\sum_{\mathbf{r}} h(\mathbf{r}) = 0. \qquad (6)$$

The AB character of the bonds is also a constant of the motion. If we start with a distribution $h(\mathbf{r})$ that is nonzero only when $\mathbf{r}$ connects sites in opposite sublattices, then $h(\mathbf{r})$ will also have this property at all subsequent τ.

A somewhat stronger property of the flow is that all weights associated with bonds of even Manhattan length $\|\mathbf{r}\| = |r_1| + |r_2| + \cdots |r_d|$, namely the AA or BB bonds, are driven to zero. This is a straightforward consequence of an asymmetry in the reconfiguration rules: (even,odd) → (even,odd), (odd,odd) → (odd,odd), and (even,even) → (odd,odd). This is yet another manifestation of the Marshall sign rule.

Accordingly, for $\tau \to \infty$ there are no bonds connecting sites in the same sublattice and all bonds have odd Manhattan length. We are thus free to impose the convention that the vector character of all bonds is directed from A to B (as anticipated in Fig. 1). This means that the bond amplitude function has a Fourier expansion

$$h(\mathbf{r}) = \frac{1}{N}\sum_{\mathbf{q}} e^{i\mathbf{q}\cdot\mathbf{r}} h_{\mathbf{q}}, \qquad (7)$$

where the wavevector sum ranges over a reduced "magnetic" Brillouin zone, equal to the standard Wigner-Seitz cell modulo $\mathbf{Q} = (\pi, \ldots \pi)$. One finds that the Fourier transform of Eq. (5) is a simple polynomial in $h_{\mathbf{q}}$,

$$\frac{1}{z}\dot{h}_{\mathbf{q}} = \gamma_{\mathbf{q}} + \gamma_{\mathbf{q}} h_{\mathbf{q}}^2 - 2h_{\mathbf{q}}, \qquad (8)$$

whose stationary distribution is

$$h_{\mathbf{q}} = \frac{1 - (1-\gamma_{\mathbf{q}}^2)^{1/2}}{\gamma_{\mathbf{q}}}. \qquad (9)$$

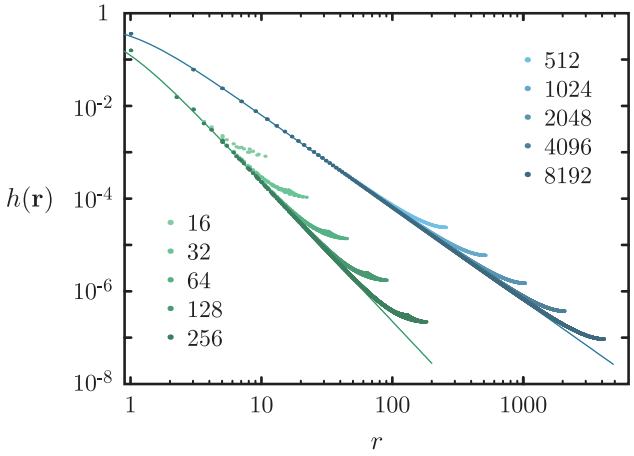

FIG. 3: The bond amplitude functions predicted for the linear-chain (upper, blue curves) and square-lattice (lower, green curves) Heisenberg models are plotted for various system sizes. Larger values of L are indicated by darker data points, following the legend. The solid lines reflect the analytical results given in Eqs. (10) and (11).

$\gamma_{\mathbf{q}} = (1/d)(\cos q_1 + \cdots \cos q_d)$ is the Fourier transform of the NN matrix. In real space, the long distance behaviour is given by

$$h(r) = \frac{2}{\pi(1+r^2)} \qquad (d=1) \qquad (10)$$

$$h(\mathbf{r}) = \frac{\sqrt{2}}{2\pi(\frac{1}{2}+r^2)^{3/2}} \qquad (d=2) \qquad (11)$$

as shown in Fig. 3. Note that in two dimensions, the bond amplitude is almost prefectly radially symmetric beyond a few lattice spacings. The general behaviour for higher dimensions is $h(\mathbf{r}) \sim (1/d + r^2)^{-(d+1)/2} \sim r^{-(d+1)}$.

III. FRUSTRATING INTERACTIONS

As we emphasized in the previous section, any model on a bipartite lattice whose interactions are nonfrustrating with respect to two-sublattice Néel order can be described in a basis consisting only of AB valence bonds.[18,46,47] Two special features of the AB basis are that (1) the overlap between any two states is strictly positive,[48] and (2) there is an exact correspondence between the Marshall sign rule and the positivity of all the RVB bond amplitudes.

We now argue that, even with the addition of frustrating interactions, one can still chose to work exclusively in the AB basis. According to Eq. (3), a frustrating interaction applied between sites in the same sublattice transforms two AB bonds into one AA and one BB bond. But since valence bonds are nonorthogonal, we can take advantage of the overcompleteness relation

$$[i,k][j,l] = [i,j][k,l] - [i,l][k,j] \qquad (12)$$

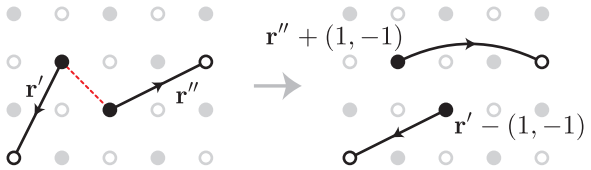

FIG. 4: A frustrating Heisenberg interaction applied between two A sublattice sites, indicated by the dotted (red) line, has the effect of exchanging the two valence bond endpoints.

to eliminate each of the unwanted bonds, yielding a new update rule

$$\Big(\frac{1}{4}+\mathbf{S}_i\cdot\mathbf{S}_k\Big)[i,l][k,j]=\frac{1}{2}[i,j][k,l], \tag{13}$$

where $i,k\in A$ and $j,l\in B$. See Fig. 4. There is no diagonal operation analogous to Eq. (3).

Following Eq. (13), a model with NN Heisenberg interactions of strengh J_1 and next-nearest-neighbour (NNN) interactions of strength J_2 has the bond amplitude master equation

$$\dot{h}(\mathbf{r})=\sum_{\mathbf{a}}\big[\delta_{\mathbf{r},\mathbf{a}}+\sum_{\mathbf{r}',\mathbf{r}''}\delta_{\mathbf{r}'+\mathbf{r}''-\mathbf{a},\mathbf{r}}h(\mathbf{r}')h(\mathbf{r}'')\big]-2zh(\mathbf{r})+\frac{J_2}{J_1}\bigg(\sum_{\tilde{\mathbf{a}}}\sum_{\mathbf{r}',\mathbf{r}''}\big[\delta_{\mathbf{r}'-\tilde{\mathbf{a}},\mathbf{r}}+\delta_{\mathbf{r}''+\tilde{\mathbf{a}},\mathbf{r}}\big]h(\mathbf{r}')h(\mathbf{r}'')-2\tilde{z}h(\mathbf{r})\bigg), \tag{14}$$

where $\tilde{\mathbf{a}}$ ranges over all NNN vectors. (We use a tilde to distinguish NNN quantities from NN ones.) This differs from Eq. (5) by a term proportional to J_2/J_1.

Fourier transformation of Eq. (14) leads to

$$\frac{1}{z}\dot{h}_{\mathbf{q}}=\gamma_{\mathbf{q}}+\gamma_{\mathbf{q}}h_{\mathbf{q}}^2-2\Big[1+g\big(1-\tilde{\gamma}_{\mathbf{q}}\big)\Big]h_{\mathbf{q}}. \tag{15}$$

This has a steady state solution

$$h_{\mathbf{q}}=\frac{\Lambda_{\mathbf{q}}-(\Lambda_{\mathbf{q}}^2-\gamma_{\mathbf{q}}^2)^{1/2}}{\gamma_{\mathbf{q}}}, \tag{16}$$

where

$$\Lambda_{\mathbf{q}}=1+g(1-\tilde{\gamma}_{\mathbf{q}})\quad\text{and}\quad g=(\tilde{z}/z)(J_2/J_1). \tag{17}$$

In dimension $d>1$, the coordination numbers are $z=2d$, $\tilde{z}=2^d$ and the connection matrices have Fourier transforms $\gamma_{\mathbf{q}}=\frac{1}{d}\sum_{k=1}^{d}\cos q_k$ and $\tilde{\gamma}_{\mathbf{q}}=\prod_{k=1}^{d}\cos q_k$.

Figure 5 illustrates the real-space distribution corresponding to Eq. (16) for several values of g in two dimensions. When $g\le 0$, the long-range behaviour is $h(\mathbf{r})\sim r^{-3}$, as in Eq. (11). When $g>0$, the radial symmetry is reduced to the C_4 symmetry of the square lattice, and the amplitudes begin to accumulate along the principle axes, especially in the $\mathbf{r}=(1,0)$ bond. Contrary to our expectations, the distribution does not become uniformly more short-ranged as g increases. Along the principle axes, it actually becomes longer-ranged: the exponent of the algebraic decay steadily decreases from 3 (at $g=0$) to 1.5 (at $g=0.5$). This looks nothing like the $h(\mathbf{r})\sim r^{-p}$ spin liquid found at $p\gtrsim 3.3$.[14,15]

The Marshall sign rule is obeyed in the J_1–J_2 model up to relatively large values of the frustration parameter.[49,50,51] At the level of approximation employed here, the bond amplitudes are all positive up to $g_M=0.323158$, the coupling at which the amplitude of the $\mathbf{r}=(2,1)$ bond passes through zero. A sign change in $h(2,1)$ at large frustration has also been observed by Lou and Sandvik in their unbiased calculation.[16]

Since there is already some ambiguity in the master equation because of the neglect of geometric constraints, we will treat g as a variational parameter. In other words, we will allow the relative weighting between the frustrating and nonfrustrating channels to deviate from $g=(\tilde{z}/z)(J_2/J_1)$, as the energy dictates.

In principle, the variational approach can be expanded to include farther-neighbour moments, defined by

$$\gamma_{\mathbf{q}}^{\boldsymbol{\mu}}=\frac{1}{d!}\sum_{\sigma\in\mathcal{S}_d}\prod_{n=1}^{d}\cos(\mu_{\sigma(n)}k_n). \tag{18}$$

Here, the index $\boldsymbol{\mu}$ is an ordered d-tuple of natural numbers, and $\mathcal{S}_d$ is the set of permutations on d elements. There will be a variational parameter $g^{\boldsymbol{\mu}}$ for each included moment, in terms of which the amplitude distribution is

$$h_{\mathbf{q}}=\frac{\lambda-\eta_{\mathbf{q}}-\big[(\lambda-\eta_{\mathbf{q}})^2-\Delta_{\mathbf{q}}^2\big]^{1/2}}{\Delta_{\mathbf{q}}}, \tag{19}$$

where

$$\eta_{\mathbf{q}}=\sum_{\text{even}}g^{\boldsymbol{\mu}}\gamma_{\mathbf{q}}^{\boldsymbol{\mu}},\quad\text{and}\quad\Delta_{\mathbf{q}}=\sum_{\text{odd}}g^{\boldsymbol{\mu}}\gamma_{\mathbf{q}}^{\boldsymbol{\mu}}. \tag{20}$$

λ is fixed by the requirement that $h_{\mathbf{q}=0}=1$. The summations in Eq. (20) are over all $\boldsymbol{\mu}$ vectors having even and odd Manhattan length up to some cutoff, $\|\boldsymbol{\mu}\|<\mu_0$. For our numerical work on the J_1–J_2 model, only the $\boldsymbol{\mu}=(1,0)$ and $\boldsymbol{\mu}=(1,1)$ components are kept.

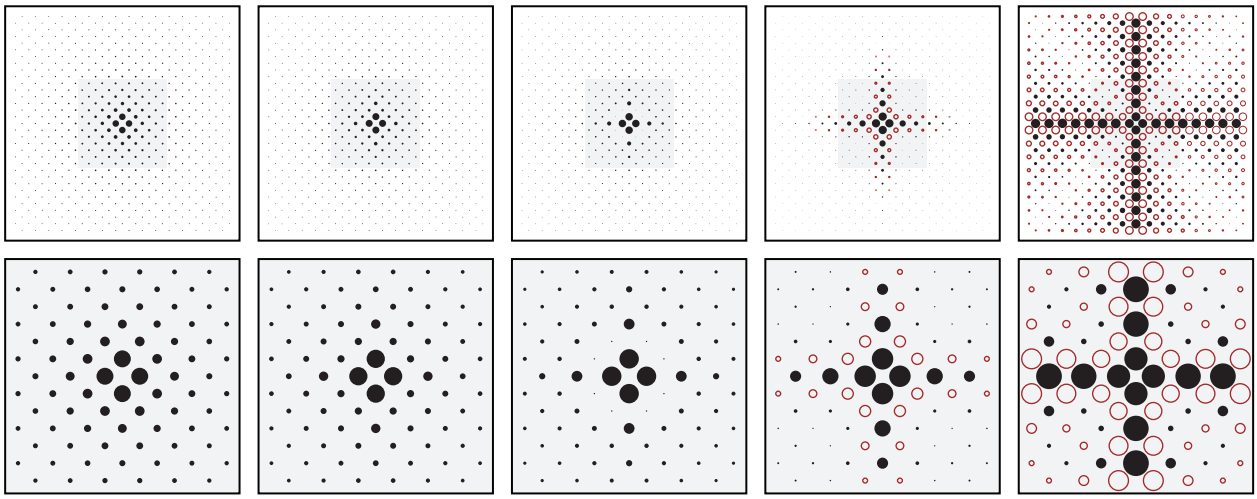

FIG. 5: The bond amplitudes $h(\mathbf{r})$ are depicted from left to right for the values $g = 0, 0.2, 0.32, 0.45, 0.49999$. The top row shows the subset of bonds up to length (16,15) for an $L = 256$ square lattice. The bottom row is a magnified view emphasizing the short range bonds up to (6,5). The position of each circle marks the endpoint of a bond whose other endpoint is at the origin. The area of each circle is proportional to $|h(\mathbf{r})|r^{3/2}$. Filled (black) circles denote a positive value and open (red) circles a negative one. For $g \leq 0$, the bond amplitudes are radially symmetric and positive definite and fall off as r^{-3}. As g increases, the distribution becomes increasingly asymmetric. The (2,1) bond steadily decreases in magnitude and vanishes at $g_M = 0.323158$. In the limit $g \to 0.5$, the bonds along the x and y axes become extremely long ranged: $h(r,0) = h(0,r) \sim r^{-3/2}$. For $g > 0.5$, the bond amplitudes are complex.

IV. RESULTS FOR THE J_1–J_2 MODEL

We work with an RVB trial wavefunction whose weights are factorized as in Eq. (1). The bond amplitudes are taken from the Fourier transform of Eq. (16). These depend only on the size of the lattice and on a single variational parameter, g, which is fixed by minimizing $E(g) = \langle \hat{H} \rangle$. Expectation values of an operator $\hat{O}$ in the trial state, written

$$\langle \hat{O} \rangle \equiv \frac{\langle h|\hat{O}|h\rangle}{\langle h|h\rangle} = \frac{\sum_{v,v'} W_{v,v'} \frac{\langle v|\hat{O}|v'\rangle}{\langle v|v'\rangle}}{\sum_{v,v'} W_{v,v'}}, \qquad (21)$$

can be interpreted as an ensemble average of the estimator $\langle v|\hat{O}|v'\rangle/\langle v|v'\rangle$ in a fluctuating gas of valence bond loops.[18,52] Over the range $g < g_M$, the bond amplitudes are all strictly positive and thus the sampling weight

$$W_{v,v'} = \langle v|v'\rangle \left[\prod h(\mathbf{r})\right]\left[\prod h(\mathbf{r}')\right] \qquad (22)$$

has no sign problem associated with it. Numerical evaluation of the RVB wavefunction is carried out using a worm algorithm[53] adapted to the valence bond loop gas.[54]

Figure 6 shows the NN and NNN spin correlations computed for finite lattices as a function of g. These data are extrapolated to the thermodynamic limit by assuming $O(L^{-3})$ leading corrections. A weighted sum of the correlations gives the variational energy:

$$E(g) = \frac{J_1}{2N} \sum_{\mathbf{r}} \left[\langle \mathbf{S}_{\mathbf{r}} \cdot \mathbf{S}_{\mathbf{r}+(1,0)} \rangle + \frac{J_2}{J_1} \langle \mathbf{S}_{\mathbf{r}} \cdot \mathbf{S}_{\mathbf{r}+(1,1)} \rangle \right]. \qquad (23)$$

The optimal value of g is found by solving $E'(g_{\min}) = 0$. The dependence of $g_{\min}$ on J_2/J_1 is shown as an inset in the bottom panel of Fig. 6. Back substitution of $g_{\min}$ into Eq. (23) gives $E(J_2/J_1)$.

As is clear from the top and middle panels of Fig. 6, a point of nonanalyticity at $g = g_M$ (or $J_2/J_1 = 0.418$) separates regions with markedly different behaviour. In the $L \to \infty$ limit, both the NN and NNN spin correlations exhibit a cusp. $E'(g)$ has no roots for $g \geq g_M$.

Figure 7 shows the staggered magnetic moment

$$M = \frac{1}{2N} \left[\sum_{\mathbf{r},\mathbf{r}'} (-1)^{\|\mathbf{r}-\mathbf{r}'\|} \langle \mathbf{S}_{\mathbf{r}} \cdot \mathbf{S}_{\mathbf{r}'} \rangle \right]^{1/2} \qquad (24)$$

plotted as both $M(g)$ and $M(J_2/J_1)$. Here, the thermodynamic limit is acheived with $O(L^{-2})$ scaling. By continuing the trend established in the region where the Marshall sign rule is obeyed, we estimate that the staggered moment vanishes continuously at a critical coupling $J_2/J_1 = 0.447$.

V. DISCUSSION

The master equation approach applied to the J_1–J_2 model leads to an RVB trial wavefunction whose bond amplitudes depend on a single variational parameter, g. Wherever the Marshall sign rule holds, we are able to compute the properties of the RVB state to very high accuracy for large lattices (up to $L = 128$ easily on a laptop) and thus to extrapolate measured values to

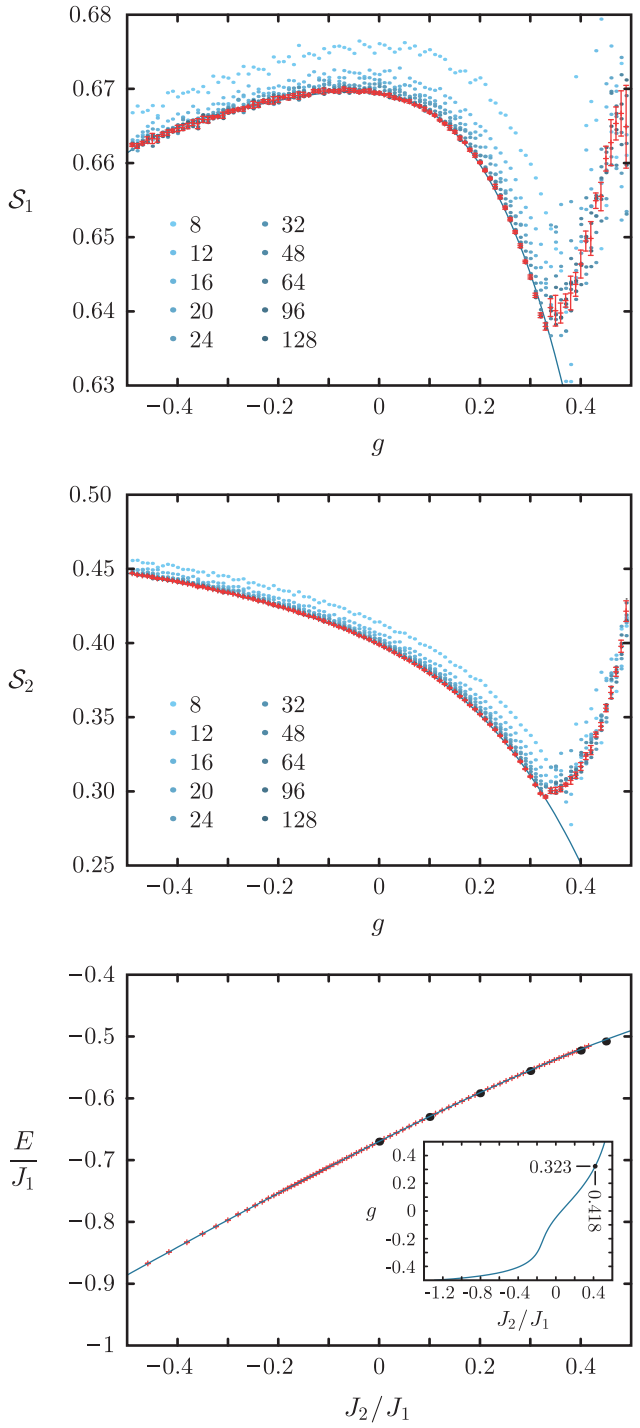

FIG. 6: (Top) The expectation value of the NN spin correlations $\mathcal{S}_1 = -(1/2N)\sum_{\mathbf{r}}\langle \mathbf{S}_{\mathbf{r}} \cdot \mathbf{S}_{\mathbf{r}+(1,0)}\rangle$ is plotted as a function of the variational parameter g. Solid circles (blue) represent data computed for a particular $L \times L$ system; see the legend. Error bars (red) denote the $L \to \infty$ extrapolation. (Middle) The NNN spin correlations $\mathcal{S}_2 = (1/2N)\sum_{\mathbf{r}}\langle \mathbf{S}_{\mathbf{r}} \cdot \mathbf{S}_{\mathbf{r}+(1,1)}\rangle$ are plotted in the same way. (Bottom) The energy density $E/J_1 = -\mathcal{S}_1 + (J_2/J_1)\mathcal{S}_2$ in the thermodynamic limit is compared to estimates (black dots) due to Gochev.[55] The inset shows the g that minimizes the variational energy.

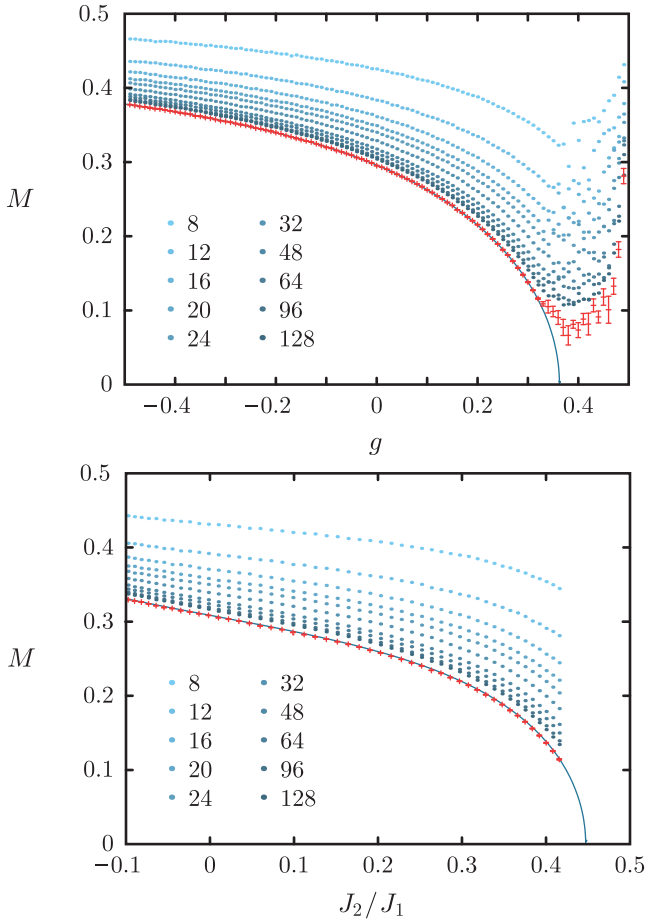

FIG. 7: (Top) The staggered magnetic moment M is plotted as a function of the variational parameter g. The dots (in shades of blue) represent data computed for a particular $L \times L$ system. Errorbars (red) indicate the extrapolated $L \to \infty$ value. The data for $g > g_M$ is unreliable for reasons elucidated in the main text. The solid line is a polynomial fit of the $L = \infty$, $g < g_M$ points. (Bottom) The $g < g_M$ data from the top panel is replotted with a new horizontal scale. The Marshall sign rule breaks down at 0.418, and the magnetic order dies at 0.447.

the thermodynamic limit. For the NN Heisenberg model ($J_2 = 0$), the energy and staggered magnetization of the best variational state (at $g = -0.0484$) extrapolate to $E = -0.669748$ and $M = 0.3086$. These differ by 0.047% and 0.52% from the exact results $E = -0.669437(5)$ and $M = 0.3070(3)$ obtained from quantum Monte Carlo.[9]

As a function of frustration, the antiferromagnetic order dies out quite slowly. When the Marshall sign rule finally breaks down (at $J_2/J_1 = 0.418$), the staggered moment has decreased only to $M = 0.1114$, about 36% of its unfrustrated value. This does not appear to be consistent with a continuous transition. One point of concensus for this model is that a gapped state appears around $J_2/J_1 \approx 0.4$. Thus, the fact that the magnetization is still large near this value suggests that the transition is first order. In comparison to other situations where a

Néel–VBS transition is known to occur,[56,57] what we observe here is much more like the situation in Ref. 56, where the staggered magnetization decreases only modestly and then collapses abruptly at a first-order critical point.

Of course, this line of reasoning is not sufficiently rigourous to establish the order of the transition, and we cannot rule out a deconfined quantum critical point. Since there are no exact results on large lattices, we do not know how well the optimized RVB wavefunction approximates the true ground state. (For 4×4 the agreement is quite good[16]: the overlap is 0.9998 for the unfrustrated case and 0.996 for $J_2/J_1 = 0.4$). We have estimated that the magnetic order vanishes at $J_2/J_1 = 0.447$ in a continuous scenario, which apparently "overshoots" the openning of the spin gap at $J_2/J_1 \approx 0.4$. It is hard to say whether these values are truly noncoincident, since their uncertainties are difficult to quantify. Moreover, the decay of the staggered magnetization may be artificially slow because of the failure of the RVB state (which is translationally invariant) to capture the incipient dimer correlations near the transition.

The sign problem in this model (for $J_2/J_1 > 0.418$) turns out not to be terribly severe. Much more catastrophic is that the master equation itself breaks down along with the Marshall sign rule, because of the assumption that $h(\mathbf{r}) \geq 0$ represents the probability of finding a bond of type $\mathbf{r}$. Once any of the amplitudes becomes negative, the reasoning that lead to Eq. (14) is no longer correct. The breakdown could perhaps be avoided if we were to use an exact numerical implementation of Eq. (2) to find the $\tau \to \infty$ limit, rather than an analytical ansatz. More likely, though, the failure of the master equation is related to the inability of the RVB state to accommodate bond-bond correlations—except indirectly by strengthening the C_4 symmetry of $h(\mathbf{r})$, as seen in Fig. 5.

The master equation approach works remarkably well in guiding our choice of the RVB bond amplitudes. Where it can be checked ($J_2 = 0$), the accuracy of the wavefunction rivals that of unbiased optimizations, but with an enormous computational saving associated with reducing the number of variational parameters from N to 1. Including variational parameters for a few additional modes (as described at the end of Sect. III) would improve the accuracy further. In order to handle the most disruptive effects of frustrating interactions, however, it will be necessary to move to the next level of approximation and to consider RVB states whose weights factorize into amplitudes for *pairs* of bonds. Obtaining an analytical master equation for the two-bond amplitude $h_{ij;kl}$, as we did in this paper for the single-bond amplitude $h_{ij} = h(\mathbf{r}_{ij})$, is probably not feasible. Nonetheless, for variational calculations, it may be enough to put in by hand some bond-bond contribution, *e.g.*,

$$h_{ij;kl} = h(\mathbf{r}_{ij})h(\mathbf{r}_{kl}) \times \big[1 + U\delta(\|\mathbf{r}_{ij} + \mathbf{r}_{kl}\|)\delta(\|\mathbf{r}_{il} + \mathbf{r}_{kj}\|)\big], \quad (25)$$

that is compatible with the expected VBS pattern (here, the columnar state at large U).

Acknowledgments

The author gives warm thanks to Anders Sandvik and Valeri Kotov for many stimulating discussions. Financial support was provided by the Alexander von Humboldt foundation.

[1] L. Pauling, Proc. R. Soc. London, Ser. A **196**, 343 (1949).
[2] P. W. Anderson, Mater. Res. Bull. **8**, 153 (1973).
[3] P. Fazekas and P. W. Anderson, Philos. Mag. **30**, 23 (1974).
[4] D. S. Rokhsar and S. A. Kivelson, Phys. Rev. Lett. **61**, 2376 (1988).
[5] R. Moessner and S. L. Sondhi, Phys. Rev. Lett. **86**, 1881 (2001).
[6] H. Bethe, Z. Phys. **71**, 205 (1931).
[7] L. Hulthén, Arkiv Mat. Astron. Fysik **26A**, No. 11 (1938).
[8] E. V. Castro, N. M. R. Peres, K. S. D. Beach, A. W. Sandvik, Phys. Rev. B **73**, 054422 (2006).
[9] A. W. Sandvik, Phys. Rev. B **56**, 11678 (1997).
[10] D. A. Huse, and U. Elser, Phys. Rev. Lett. **60**, 2531 (1988).
[11] R. R. P. Singh and D. A. Huse, Phys. Rev. Lett. **68**, 1766 (1992).
[12] L. Capriotti, A. E. Trumper, and S. Sorella, Phys. Rev. Lett. **60**, 3899 (1999).
[13] The existence of long range magnetic order depends on the proliferation of loops[18] formed by the overlap of valence bond configurations,[48] and for purely geometric reasons bonds of finite range cannot form system-spanning loops in dimensions $d < 3$.[15]
[14] S. Liang, B. Doucot, and P. W. Anderson, Phys. Rev. Lett. **61**, 365 (1988).
[15] K. S. D. Beach, arXiv:0707.0297v1 (unpublished).
[16] J. Lou and A. W. Sandvik, arXiv:cond-mat/0605034v3 (unpublished).
[17] The factorizable form can be justified by a mean field decomposition of the Heisenberg hamiltonian in terms of bond operators. The amplitudes $h(\mathbf{r})$ are predicted to decay as $1/r^{d+1}$; see Ref. 15.
[18] K. S. D. Beach and A. W. Sandvik, Nucl. Phys. B **750**, 142 (2006).
[19] P. Chandra and B. Doucot, Phys. Rev. B **38**, 9335 (1988).
[20] F. Figueirido *et al.*, Phys. Rev. B **41**, 4619 (1989).
[21] T. Oguchi and H. Kitatani, J. Phys. Soc. Jpn. **59**, 3322 (1990).
[22] H. J. Schulz and T. A. L. Ziman, Europhys. Lett. **18**, 355 (1992).
[23] Guang-Ming Zhang, Hui Hu, and Lu Yu, Phys. Rev. Lett. **91**, 067201 (2003).

[24] E. Dagotto *et al.*, Phys. Rev. Lett. **63**, 2148 (1989).
[25] M. P. Gelfand, R. R. P. Singh, and D. A. Huse, Phys. Rev. B **40**, 10801 (1989).
[26] M. P. Gelfand *et al.*, Phys. Rev. B **42**, 8206 (1990).
[27] R. R. P. Singh and R. Narayan, Phys. Rev. Lett. **65**, 1072 (1990).
[28] M. Zhitomirsky and K. Ueda, Phys. Rev. B **54**, 9007 (1996).
[29] L. Capriotti and S. Sorella, Phys. Rev. Lett. **84**, 3173 (2000).
[30] M. Mambrini, A. Läuchli, D. Poilblanc, and F. Mila, Phys. Rev. B **74**, 144422 (2006).
[31] H. J. Schulz, T. A. L. Ziman, and D. Poilblanc, J. Phys. I (France) **18**, 355 (1992).
[32] V. N. Kotov, J. Oitmaa, O. P. Sushkov, and Z. Weihong, Phys. Rev. B **60**, 14613 (1999).
[33] V. B. Kotov and O. P. Sushkov, Phys. Rev. B **61**, 11820 (2000).
[34] J. Oitmaa and Z. Weihong, Phys. Rev. **54**, 3022 (1996).
[35] R. R. P. Singh, W. H. Zheng, C. J. Hamer, and J. Oitmaa, Phys. Rev. B **60**, 7278 (1999).
[36] S. Sorella, Phys. Rev. Lett. **80**, 4558 (1998).
[37] V. N. Kotov, J. Oitmaa, O. P. Sushkov, and Z. Weihong, Philos. Mag. A **80**, 1483 (2000).
[38] T. Senthil, A. Vishwanath, L. Balents, S. Sachdev, and M. P. A. Fisher, Science **303**, 1490 (2004); T. Senthil, L. Balents, S. Sachdev, A. Vishwanath, and M. P. A. Fisher, Phys. Rev. B **70**, 144407 (2004).
[39] V. N. Kotov, D. X. Yao, A. H. Castro Neto, and D. K. Campbell, arXiv:0704.0114v1 (unpublished).
[40] J. Sirker, Z. Weihong, O. P. Sushkov, and J. Oitmaa, Phys. Rev. B **73**, 184420 (2006).
[41] A. Chubukov, Phys. Rev. B **44**, 392 (1991).
[42] G. Rumer, Gottingen Nachr. Tech. **1932**, 377 (1932).
[43] L. Pauling, J. Chem. Phys. **1**, 280 (1933).
[44] W. Marshall, Proc. Roy. Soc. (London) **A232**, 48 (1955).
[45] Anders W. Sandvik and K. S. D. Beach, proceedings of "Computer Simulation Studies in Condensed Matter Physics XX"; arXiv:0704.1469v1.
[46] F. Alet, S. Capponi, N. Laflorencie, M. Mambrini, Phys. Rev. Lett. **99**, 117204 (2007).
[47] M. Mambrini, arXiv:0706.2508v2 (unpublished).
[48] B. Sutherland, Phys. Rev. B **37**, 3786 (1988).
[49] J. Richter, N. B. Ivanov, and K. Retlaff, Europhys. Lett. **25**, 545 (1994).
[50] N. B. Ivanov and J. Richter, J. Phys.: Condens. Matter **6** 3785 (1994).
[51] A. Voigt, J. Richter, and N. B. Ivanov, Physica A **245**, 269 (1997).
[52] A. W. Sandvik, Phys. Rev. Lett. **95**, 207203 (2005).
[53] N. Prokof'ev and B. Svistunov, Phys. Rev. Lett. **87**, 160601 (2001).
[54] K. S. D. Beach, unpublished.
[55] I. G. Gochev, Phys. Rev. B **49**, 9594 (1994)
[56] K. S. D. Beach and Anders W. Sandvik, Phys. Rev. Lett. **99**, 047202 (2007).
[57] Anders W. Sandvik, Phys. Rev. Lett. **98**, 227202 (2007).